

# Interband Cascade (IC) Optical Frequency Combs

Mahmood Bagheri<sup>1</sup>, Clifford Frez<sup>1</sup>, Igor Vurgaftman<sup>2</sup>, Mathieu Fradet<sup>1</sup>, Ivan Grudinin<sup>1</sup>, Chadwick L. Canedy<sup>2</sup>, William W. Bewley<sup>2</sup>, Charles D. Merritt<sup>2</sup>, Chul Soo Kim<sup>2</sup>, Siamak Forouhar<sup>1</sup> and Jerry R. Meyer<sup>2</sup>

<sup>1</sup>Jet Propulsion Laboratory, California Institute of Technology, Pasadena, CA 91109, USA

<sup>2</sup>Naval Research Laboratory, Washington, DC 20375, USA

**We demonstrate an electrically-driven frequency comb whose sub-picosecond pulses span more than 1 THz of spectral bandwidth centered near 3.6  $\mu\text{m}$ . This is achieved by passively mode locking an interband cascade laser with gain and saturable absorber sections monolithically integrated on the same chip.**

**Index Terms**—Interband cascade laser, mode-locked laser, optical frequency combs.

## I. INTRODUCTION

**O**PTICAL frequency combs in the visible to near-infrared range of the electromagnetic spectrum have quickly become standards for precise measurements of frequency and time [1], besides having revolutionized precision spectroscopy [2], [3]. The extension of frequency combs into the midwave infrared (mid-IR) has broad implications for molecular composition spectroscopy, since numerous molecules undergo strong vibrational transitions in this range. Optical combs can provide precision spectroscopy [4], [5], with large dynamic range in real-time. In particular, mid-IR combs can be exploited to detect small traces of environmental and toxic agents in atmospheric, security, and industrial applications, because a mid-IR beam can propagate over long distances in the earth's atmosphere with small attenuation. To date, most mid-IR combs have been realized via frequency down-conversion of a near-IR comb through optical parametric oscillation [6] or difference frequency generation [7], [8] or by continuous wave (cw) optical pumping of a micro-resonator [9]. Beyond 7  $\mu\text{m}$ , frequency combs based on four-wave mixing in quantum cascade lasers (QCLs) have recently produced high output powers with wide optical bandwidth [10], [11]. However, QCL performance degrades in the 3-4  $\mu\text{m}$  band where a large fraction of the absorption features associated with C-H bonds are clustered. By mode locking a new class of semiconductor laser, we have demonstrated the first electrically pumped optical frequency combs to operate in the 3-4  $\mu\text{m}$  wavelength range. The combs generate sub-picosecond pulses at gigahertz repetition rates [12].

## II. EXPERIMENT

A split-contact gain/saturable-absorber architecture [13], in which the top metal contact of the ICL is divided into a longer forward-biased portion, and a relatively-shorter reverse-biased portion that functions as a saturable absorber (SA), is employed to realize mode-locking. The saturable absorber drives the multimode operation and phase locks the longitudinal modes of the ICL cavity. Figure 1(a) illustrates the 4-mm-long laser cavity with split contacts that was used in this study. The ICL wafer with 7 active stages was grown by molecular

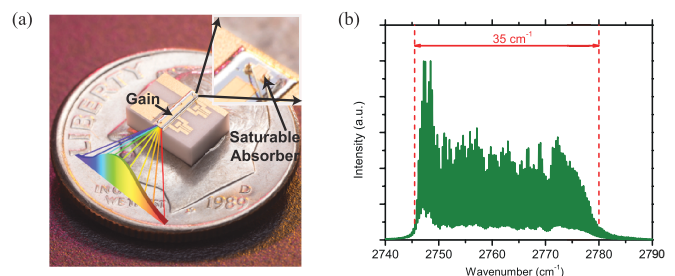


Fig. 1. (a) A 4mm-long ICL mode-locked laser consisting of gain (front) and saturable absorber (back) sections, (b) FTIR spectrum of the mode-locked ICL operating at  $I = 325$  mA and  $T = 15^\circ\text{C}$  with the SA junction left open, showing  $>35$   $\text{cm}^{-1}$  (1.05 THz) bandwidth and  $>120$  modes.

beam epitaxy on an n-GaSb substrate, using design and growth procedures similar to those discussed previously [14]. The laser cavity features a 200- $\mu\text{m}$ -long saturable absorber section that is separated from the gain section by a non-contacted 100- $\mu\text{m}$ -long gap to prevent electrical shorting of the two sections. For this architecture to be effective, the material gain recovery time ( $\tau_g$ ) should exceed the cavity round trip time,  $\tau_{RT}$ , which is satisfied in an ICL due to the long carrier lifetime for interband transitions ( $\tau_g \approx 500$  ps, vs.  $\tau_{RT} \approx 100$  ps for a while long cavity) [15]. Furthermore, the time required for the SA section to recover strong absorption ( $\tau_{abs}$ ) should be shorter than the gain recovery time. These conditions open an amplification window around the pulse because rapid absorption recovery shortens the leading edge of the pulse. While the same process can also shorten the trailing edge if  $\tau_{abs}$  is shorter than the pulse width, the present devices do not fall in the fast SA regime.

Several schemes are commonly used to accelerate the absorption recovery in a mode-locked diode laser that monolithically incorporates a saturable absorber. These include ion implantation and the use of a split contact to reverse bias the SA section. In our demonstration,  $\tau_{abs}$  was reduced by implanting high-energy  $\text{H}^+$  ions. A split contact was also patterned to allow separate biasing of the SA section, although that feature was not used in the experiments reported here and the SA junction was left open.

Under dc bias, the laser operates at  $T = 15^\circ\text{C}$  with a

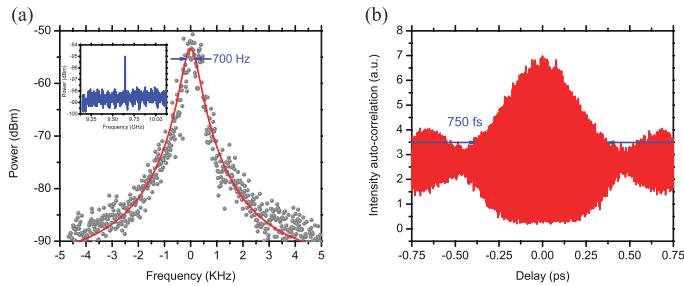


Fig. 2. (a) RF beat-note with 700 Hz linewidth. The inset shows the RF tone at 9.68 GHz on a much broader scale, (b) Intensity autocorrelation trace shows that the mode-locked ICL emits pulses of width  $\approx 750$  fs.

threshold of  $I_{th} = 85$  mA. Although just above threshold the emission is into a single longitudinal mode, at higher currents the spectrum broadens ( $>1$  THz) and becomes multi-mode. Figure 1(b) shows the lasing spectrum at 325 mA and  $15^\circ\text{C}$ , as acquired by a Fourier transform infrared (FTIR) spectrometer. The overall bandwidth is  $35\text{ cm}^{-1}$  (52 nm). The comb emission comprises over 120 modes, with  $>50\ \mu\text{W}$  of power in each mode.

In this geometry the saturable absorber section functions as a fast optical detector that produces an electrical RF tone useful to analyze the laser performance and synchronize external events. The same Fabry-Perot cavity with no coupling among its axial modes will display an RF tone near the round-trip frequency with  $>1$  MHz linewidth due to relative phase fluctuations of the incoherent modes. However, Fig. 2(a) shows a far narrower RF spectrum with linewidth only 700 Hz for the multi-section ICL operating at  $I = 325$  mA. The narrow linewidth, large signal-to-noise ratio, and stability of this beat note confirm that mode locking has been achieved, with negligible random drift of the relative phases of the  $>120$  modes lasing simultaneously in the cavity.

Under mode-locked conditions, the axial modes in the Fabry-Perot cavity combine coherently to generate very short optical pulses. We have employed second-order autocorrelation to analyze the temporal characteristics of the pulses. In this measurement, the optical pulse is combined with its delayed replica, and the combined beam is sent collinearly into an extended InGaAs photodiode in which it is detected by two-photon absorption. While the laser photon energy corresponding to  $\lambda = 3.6\ \mu\text{m}$  (0.34 eV) is insufficient to bridge the detector bandgap of 0.59 eV, two-photon absorption in the InGaAs generates a second-order autocorrelation spectrum. Figure 2(b) shows the measured second-order autocorrelation for the mode-locked ICL operated at  $I = 325$  mA and  $T = 15^\circ\text{C}$ . The autocorrelation spectrum shows a strong peak at zero delay, which is expected since with no delay the two beams should overlap perfectly. The full-width at half maximum (FWHM) of the narrow peak is less than 1 ps. That the interferogram signal does not disappear entirely outside the main peak implies the presence of parasitic modes that are not phase-locked to the rest of the modes traveling in the cavity.

### III. CONCLUSION

In summary, we have demonstrated the first passively mode-locked mid-IR semiconductor lasers. The electrically-pumped interband cascade devices with gain and saturable absorber sections monolithically patterned onto the same ridge emit near  $3.6\ \mu\text{m}$ , with a frequency comb bandwidth of  $35\text{ cm}^{-1}$ . For operation with a dc bias at  $15^\circ\text{C}$ , the pulse length is  $<1$  ps and the RF beat-note linewidth is  $<1$  kHz. The beating of two combs with slightly different repetition frequencies is also demonstrated. This new capability offers unique opportunities for broadband laser spectroscopy to probe the strong fingerprint absorption lines of numerous chemical and biological agents. A focus of future work will be to increase the spectral width of the comb output, by using chirped quantum-well thicknesses in the ICL active stages to broaden the gain spectrum and by mitigating the potentially deleterious effect of group velocity dispersion.

### ACKNOWLEDGMENT

This work was supported under the Defense Advanced Research Project Agency (DARPA) SCOUT program and performed at the Jet Propulsion Laboratory (JPL), California Institute of Technology, under contract with the NASA.

### REFERENCES

- [1] Udem, T., Holzwarth, R. & Hansch, T. W. Optical frequency metrology. *Nature* **416**, 233–237 (2002).
- [2] Keilmann, F., Gohle, C. & Holzwarth, R. Time-domain mid-infrared frequency-comb spectrometer. *Opt. Lett.* **29**, 1542–1544 (2004).
- [3] Coddington, I., Swann, W. C. & Newbury, N. R. Coherent multiheterodyne spectroscopy using stabilized optical frequency combs. *Physical Review Letters* **100**, 013902 (2008).
- [4] Nugent-Glandorf, L. *et al.* Mid-infrared virtually imaged phased array spectrometer for rapid and broadband trace gas detection. *Opt. Lett.* **37**, 3285–3287 (2012).
- [5] Fleisher, A. J. *et al.* Mid-infrared time-resolved frequency comb spectroscopy of transient free radicals. *The Journal of Physical Chemistry Letters* **5**, 2241–2246 (2014).
- [6] Lee, K. F. *et al.* Frequency combs for cavity cascades: Opo combs and graphene-coupled cavities. *Journal of Physics B: Atomic, Molecular and Optical Physics* **50**, 014003 (2016).
- [7] Foreman, S. M., Jones, D. J. & Ye, J. Flexible and rapidly configurable femtosecond pulse generation in the mid-ir. *Opt. Lett.* **28**, 370–372 (2003).
- [8] Cruz, F. C. *et al.* Mid-infrared optical frequency combs based on difference frequency generation for molecular spectroscopy. *Opt. Express* **23**, 26814–26824 (2015).
- [9] Wang, C. Y. *et al.* Mid-infrared optical frequency combs at  $2.5\ \mu\text{m}$  based on crystalline microresonators. *Nature communications* **4**, 1345 (2013).
- [10] Hugi, A., Villares, G., Blaser, S., Liu, H. & Faist, J. Mid-infrared frequency comb based on a quantum cascade laser. *Nature* **492**, 229–233 (2012).
- [11] Lu, Q., Wu, D., Slivken, S. & Razeghi, M. High efficiency quantum cascade laser frequency comb. *Scientific Reports* **7**, 43806 (2017).
- [12] Bagheri, M. *et al.* Passively mode-locked interband cascade optical frequency combs. *Scientific Reports* **8**, 3322 (2018).
- [13] Williams, K., Thompson, M. & White, I. Long-wavelength monolithic mode-locked diode lasers. *New Journal of Physics* **6**, 179 (2004).
- [14] Canedy, C. L. *et al.* Pulsed and cw performance of 7-stage interband cascade lasers. *Opt. Express* **22**, 7702–7710 (2014).
- [15] Avrutin, E., Marsh, J. & Portnoi, E. Monolithic and multi-gigahertz mode-locked semiconductor lasers: constructions, experiments, models and applications. *IEE Proceedings-Optoelectronics* **147**, 251–278 (2000).